High-pressure synthesis, characterization, and equation of state of double perovskite Sr_2CoFeO_6*

Pan Yue-Wu(潘跃武)[a], Zhu Pin-Wen(朱品文)[b], and Wang Xin(王 欣)[b]†

[a] Mathematics and Physical Sciences Technology, Xuzhou Institute of Technology, Xuzhou 221018, China
[b] State Key Laboratory of Superhard Materials, Jilin University, Changchun 130012, China

(Received 19 July 2014; revised manuscript received 22 September 2014; published online 25 November 2014)

Double perovskite oxide Sr_2CoFeO_6 (SCFO) has been obtained using a high-pressure and high-temperature (HPHT) synthesis method. Valence states of Fe and Co and their distributions in SCFO were examined with X-ray photoelectron spectroscopy. The electric transport behavior of SCFO showed a semiconductor behavior that can be well described by Mott's law for variable-range hopping conduction. The structural stability of SCFO was investigated at pressures up to 31 GPa with no pressure-induced phase transition found. Bulk modulus B_0 was determined to be 163(2) GPa by fitting the pressure–volume data to the Birch–Murnaghan equation of state.

Keywords: double perovskite oxide, electric properties, high pressure

PACS: 75.47.Lx, 61.05.cp, 64.60.–i **DOI:** 10.1088/1674-1056/24/1/017503

1. Introduction

Double perovskite oxides of general formula $A_2BB'O_6$ (A = divalent alkaline earth ions; B and B' = transition metal ions) have been extensively studied because they present interesting magnetic and transport properties. Especially, the mixed-valent molybdenum perovskite (Sr_2FeMoO_6) exhibits colossal magnetoresistance,[1] and the copper oxide ($Sr_2YRu_{0.95}Cu_{0.05}O_6$) shows superconductivity.[2] In either case, the special physical properties are strongly related to the charge ordering phenomena and the couplings among lattice, orbital, and spin degrees of freedom.

Among those oxides, Co-based double perovskite oxides have attracted a lot of attention and shown a wide range of intriguing properties, e.g., antiferromagnetism, ferromagnetism,[3–9] spin-glass behavior,[10] and magnetoresistance.[11] Sr_2CoMoO_6 is an insulating antiferromagnet with electronic configuration $Co^{2+}(3d^7)$–$Mo^{6+}(4d^0)$. This configuration requires a completely unquenched orbital contribution for the high spin (HS) Co^{2+} cation, which explains the large effective moment of $5.3\mu_B$ obtained in the paramagnetic region well above T_N.[11] By substituting Mo with Fe, the different valence states of Co and Fe may have interesting impacts on the magnetic and transport properties of the new oxide. To the best of our knowledge, only a few studies on Sr_2CoFeO_6 have been reported.[10,12,13] The previous study on Sr_2CoFeO_6 showed that Fe and Co were both in tetravalent oxidation states, and the HS states of Co^{4+} ($d^5\bar{L}$) and Fe^{4+} ($d^4\bar{L}$) could lead to metallicity and ferromagnetism.[14] However, some other research showed that in Sr_2CoFeO_6, Fe and Co were in mixed valence states of +3 and +4, and inferred that Co^{3+} was in an intermediate spin state while Fe^{3+}, Fe^{4+}, and Co^{4+} were in low spin states.[10]

In recent studies, temperature- and pressure-induced structural changes have been observed in Co-based double perovskite oxides. For example, the structure of Sr_2CoSbO_6 would transform from trigonal ($R\bar{3}$) to cubic ($Fm\bar{3}m$) above 470 K;[15] Sr_2CoTeO_6 undergoes a phase transition from cubic ($Fm\bar{3}m$) to monoclinic ($I2/m$) above 773 K;[16,17] La_2CoMnO_6 transforms from monoclinic ($P2_1/n$) to rhombohedral ($R3$) above 598 K;[18] and Sr_2CoReO_6 would transform from tetragonal ($I4/m$) to monoclinic ($P2_1/n$) with decreasing temperature.[19] Sr_2CoWO_6 shows two phase transitions: a first transition from monoclinic ($P2_1/n$) to tetragonal ($I4/m$) at 258 K, then a second transition to cubic ($Fm\bar{3}m$) followed at 703 K.[20,21] Similar successive phase transitions have also been reported for Pb_2CoTeO_6: the transitions from cubic ($Fm\bar{3}m$) to rhombohedral ($R\bar{3}$) then to monoclinic ($I2/m$) and to monoclinic ($P2_1/n$) occur at 370 K, 210 K, and 125 K, respectively; afterwards it remains stable down to 5 K.[22] On the other hand, the pressure is also shown to have a strong influence on these oxides. For example, Sr_2CoWO_6 transforms from tetragonal ($I4/m$) to monoclinic ($P2_1/n$) at 2.2 GPa.[23] While some Co-based double perovskite oxides are found to be structurally stable under high pressures, like Sr_2CoMoO_6 with no pressure-induced phase transition up to 6.3 GPa.[24] In order to examine the valence states of Fe and Co ions and the structural stability, we investigate the valence states of Fe and Co ions and their respective distributions in Sr_2CoFeO_6 (SCFO). The magnetoresistance effect and the high-pressure

*Project supported by the National Natural Science Foundation of China (Grant Nos. 51172194 and 51172091), the Program for New Century Excellent Talents in University, China (Grant No. NCET-12-0240), and Jilin Province Science and Technology Development Program, China (Grant No. 20130101023JC).

†Corresponding author. E-mail: xin_wang@jlu.edu.cn

© 2015 Chinese Physical Society and IOP Publishing Ltd

behavior in Sr_2CoFeO_6 are studied.

2. Experiment

2.1. Sample preparation

The precursor of Sr_2CoFeO_6 was prepared by the sol–gel method with citric acid as a complexant. Stoichiometric $Sr(NO3)_2$, $Co(NO_3)_2{\cdot}6H_2O$, and $Fe(NO_3)_3{\cdot}9H_2O$ of analytical grade were dissolved in water, and then citric acid and ethylene glycol were added. The mixed solution was slowly evaporated at 80–90 °C until a gel was formed. Subsequently, the gel was dried at 130 °C and then heated at 850 °C in air for 10 h. After being uniformly ground in an agate mortar, the mixture was pressed into a disk with a diameter of 8 mm and a thickness of 2 mm. The disk-shaped samples were assembled for the high-pressure and high-temperature (HPHT) synthesis in a cubic anvil high-pressure apparatus at 1473 K and 5 GPa for 1 h.

2.2. X-ray diffraction measurement

The crystal structure and the phase purity of Sr_2CoFeO_6 were examined using conventional X-ray powder diffraction at room temperature. X-ray diffraction (XRD) measurement was performed using a Rigaku Rotaflex X-ray diffractometer with Cu K_α radiation in the range of 20°–80°. High-pressure angle dispersive XRD measurement was performed at beamline 3W1A of the Institute of High Energy Physics, CAS.

2.3. X-ray photoelectron spectroscopy measurement

X-ray photoelectron spectroscopy (XPS) measurements were performed with an ESCALAB 250 spectrometer using an Al K_α X-ray source. The obtained binding energies were standardized and analyzed using C_{1s} as the reference at 284.9 eV.

2.4. Electric resistivity measurement

Measurements of the electric resistivity were performed with the four-point probe method from 10 K to 300 K under an applied magnetic field of 8 T in a commercial Quantum Design physical property measurement system (PPMS).

3. Results and discussion

3.1. Crystal structure

At ambient pressure, Sr_2CoFeO_6 is found to have a cubic crystal structure (space group Fm-$3m$). As shown in Fig. 1, it can be viewed as a regular arrangement of the corner-sharing CoO_6 and FeO_6 octahedra, alternating along the crystal axes, with the large Sr cations occupying the voids between CoO_6 and FeO_6 octahedra. The X-ray diffraction pattern at the ambient condition is displayed in Fig. 2, and the calculated lattice parameter $a = 7.7323(5)$ Å is in good agreement with the previous reports.[12,25]

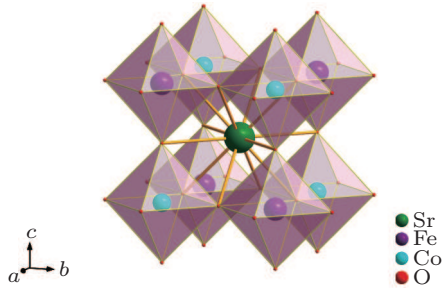


Fig. 1. (color online) Crystal structure of Sr_2CoFeO_6.

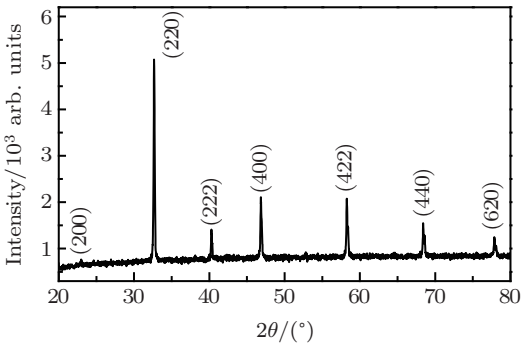


Fig. 2. X-ray diffraction pattern of Sr_2CoFeO_6 at the ambient condition.

3.2. XPS measurements

Figure 3 shows the results of XPS measurements on Fe 2p and Co 2p in Sr_2CoFeO_6. Lorenz–Gaussian fitting of the peaks to the components of Fe^{3+}, Fe^{4+}, Co^{3+}, and Co^{4+} is also given in the figure. The relative peak intensities of the fitting curves are summarized in Table 1. The peaks at 712.51 eV and 725.63 eV identify the existence of Fe^{4+}; those at 710.56 eV and 723.64 eV identify the existence of Fe^3. The binding energies of 780.59 eV and 795.77 eV correspond to Co^{3+}; while those of 781.66 eV and 797.55eV correspond to Co^{4+}. These results are in good agreement with the previous reported values.[26,27]

According to the XPS spectral analysis, it can be deduced that in Sr_2CoFeO_6, the B sites are randomly occupied by Fe and Co in the mixed valence states of Fe^{3+}/Fe^{4+} or Co^{3+}/Co^{4+}. Owing to the coexistence of Fe^{4+}, Fe^{3+}, Co^{4+}, and Co^{3+}, in order to maintain electric neutrality of Sr_2CoFeO_6, there should be some oxygen vacancies inside Sr_2CoFeO_6. Such oxygen vacancies induced by the random occupancy and the mixed valence may account for the observed spin glass behavior, which is caused by the inhomogeneous magnetic exchange interactions.[10]

Table 1. Relative XPS peak intensities of Fe^{3+}, Fe^{4+} , Co^{3+}, and Co^{4+} components.

Component	Fe^{3+}	Fe^{4+}	Co^{3+}	Co^{4+}
Intensity/%	57.73	42.27	46.52	53.48

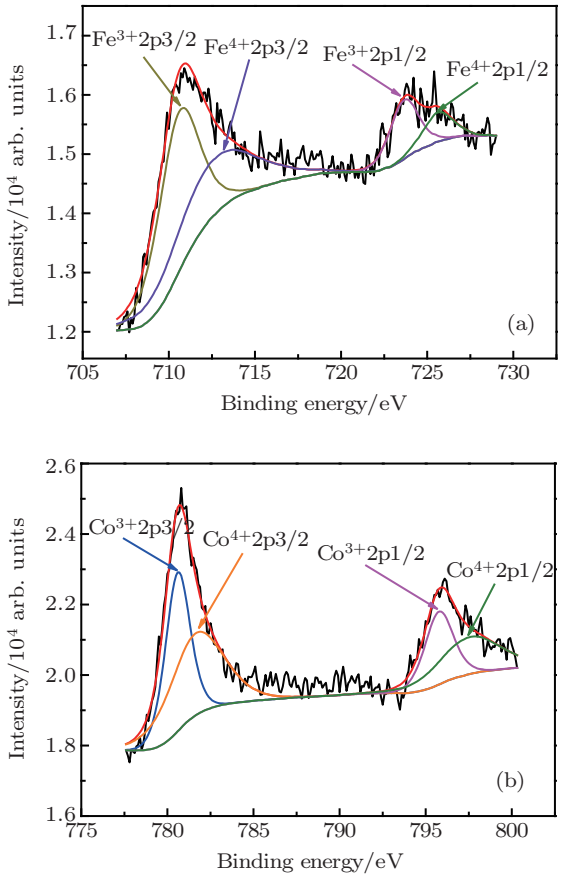


Fig. 3. (color online) XPS spectra of (a) Fe 2p and (b) Co 2p in Sr_2CoFeO_6.

3.3. Electric resistivity measurements

The electric resistance of SFCO in 0 T and 8 T applied magnetic fields is presented in Fig. 4. It exhibits a monotonic increase with decreasing temperature, and the variation of the electric resistance indicates a semiconducting behavior.

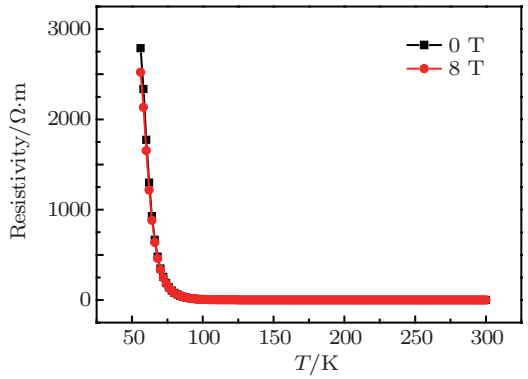


Fig. 4. (color online) Temperature dependence of the electric resistance of Sr_2CoFeO_6 in 0 T and 8 T.

As shown in Fig. 4, unlike Sr_2CoMoO_6, the resistivity curves measured in the fields of 0 T and 8 T are almost identical, indicating that Sr_2CoFeO_6 has a negligible magnetoresistance.

In order to understand the electric transport properties of Sr_2CoFeO_6, the resistivity data are fitted to various models, among which the Mott variable-range hopping (MVRH) model[28–30] is the best fit to our results, as shown in Fig. 5. The Mott variable-range hopping model gives the temperature-dependent resistivity as follows: $\rho=\rho_o \exp(T_o/T)^x$, with exponent $x = 1/4$, as expected in three dimensions. The best fitted values are $T_o = 3.10\times10^8$ K, $\rho_o = 1.34\times10^{-14}$ Ω·m (at 0 T) and $T_o = 3.06\times10^8$ K, $\rho_o = 1.51\times10^{-14}$ Ω·m (at 8 T), where T_o is related to the localization length ξ with the relationship $kT_o=\frac{18}{N(E_F)\xi^3}$, and $N(E_F)$ denotes the density of states at the Fermi level. It suggests that the resistivity is not only induced by the thermally activated mechanism of carrier hopping, and there is no energy gap opening for the upturn of resistance at low temperature.

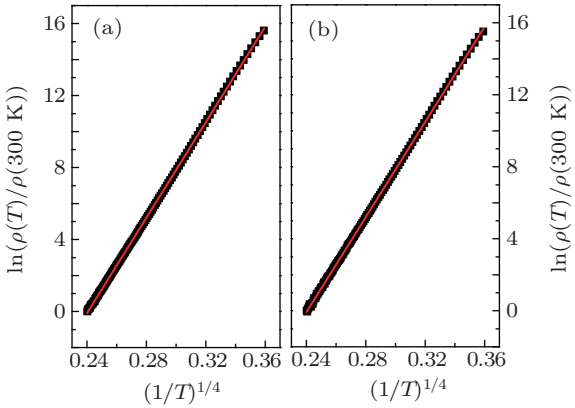


Fig. 5. (color online) $\ln\rho(T)$ versus $(1/T)^{1/4}$ normalized to the resistivity at 300 K ($\ln(\rho(T)/\rho(300\,\mathrm{K}))$) of Sr_2CoFeO_6 in (a) 0 T and (b) 8 T. The red lines are linear fits to the experimental data, indicating that the 3D variable range hopping mechanism is valid in the measured temperature range.

3.4. High pressure X-ray diffraction measurements

Various compounds in the double perovskite family are found to have different high pressure behaviors.[23,24] Further investigations of the structural stability in these compounds would be beneficial for understanding their physical properties at high pressures. This study reports a high pressure X-ray diffraction study of Sr_2CoFeO_6. Figure 6 shows the X-ray diffraction patterns at various pressures up to 31.0 GPa. The lowest diffraction pattern is indexed with respect to the cubic phase and some impurity (unreacted oxides) peaks existing in the pattern are marked by asterisks. All the X-ray diffraction peaks shift toward higher 2θ values, and no new peaks are found with increasing pressure. The variation of the relative intensities and the broadening of the X-ray diffraction peaks upon compression can be attributed to the thinning of the sample and the uniaxial compression in the process. We thus conclude that no structural phase transition has occurred up to the highest pressure.

The lattice parameter a and the unit cell volume as a function of pressure are plotted in Fig. 7. The second order Birch–Murnaghan equation of state (BM-EoS) is applied to determine the bulk modulus.[31] The fitting gives the bulk modulus

$B_o = 163(2)$ GPa. The lattice parameter and the unit cell volume of Sr_2CoFeO_6 decrease smoothly with increasing pressure, with no evidence of any phase transition throughout the whole pressure range.

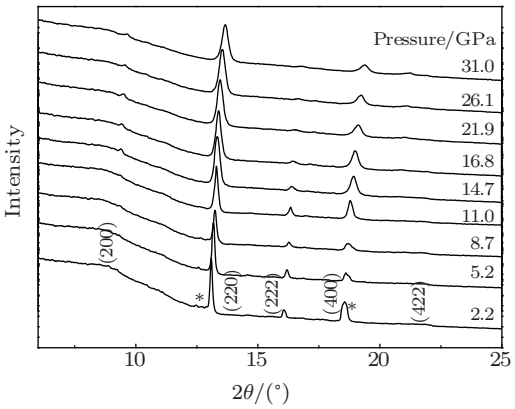


Fig. 6. Selected X-ray diffraction patterns of Sr_2CoFeO_6 at room temperature for various pressures from 2.2 GPa to 31.0 GPa. Some impurity (unreacted oxides) peaks are marked by asterisks. The wavelength λ is 0.6199 Å. In the whole pressure range, the crystal structure of Sr_2CoFeO_6 remains cubic.

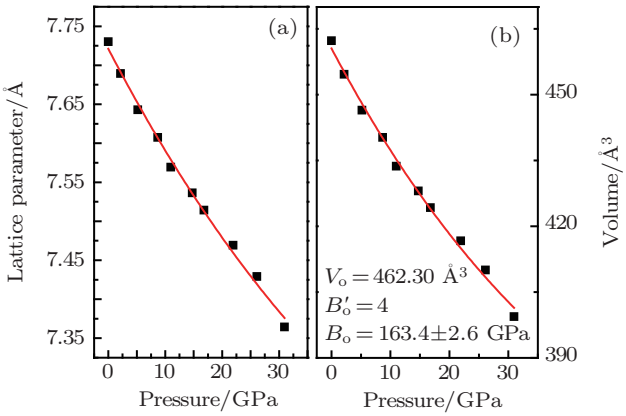


Fig. 7. (color online) (a) Lattice parameters of cubic Sr_2CoFeO_6 versus pressure up to 31.0 GPa at room temperature. (b) Pressure dependence of unit cell volumes and data fitting using BM-EoS.

4. Conclusion

Double perovskite Sr_2CoFeO_6 has been successfully prepared by the HPHT method. Using X-ray photoelectron spectroscopy, we confirm the existence of different valence states of Fe and Co ions, and their random distributions in the lattice of Sr_2CoFeO_6 are also shown. The resistivity measurements show that Sr_2CoFeO_6 is a Mott variable-range hopping semiconductor with a large T_o of 3.06×10^8 K and it exhibits a negligible magnetoresistance in a magnetic field of 8 T. *In situ* synchrotron X-ray diffractions of Sr_2CoFeO_6 have been performed at pressures up to 31.0 GPa in a diamond anvil cell. The crystal structure of this compound remains cubic in the whole pressure range. The bulk modulus of Sr_2CoFeO_6 is determined to be 163(2) GPa.

References

[1] Kobayashi K I, Kimura T, Sawada H, Terakura K and Tokura Y 1998 *Nature* **395** 677
[2] DeMarco M, Blackstead H A, Dow J D, Wu M K, Chen D Y, Chien F Z, Haka M, Toorongian S and Fridmann J 2000 *Phys. Rev. B* **62** 14301
[3] Kato H, Okuda T, Okimoto Y, Tomioka Y, Oikawa K, Kamiyama T and Tokura Y 2004 *Phys. Rev. B* **69** 184412
[4] Phatak R, Krishnan K, Sali S K, Das A and Nigam A K 2013 *J. Magn. Magn. Mater.* **344** 129
[5] Murthy J K and Venimadhav A 2013 *J. Appl. Phys.* **113** 163906
[6] Pradheesh R, Nair H S, Sankaranarayanan V and Sethupathi K 2012 *Eur. Phys. J. B* **85** 260
[7] Martinez-Lope M J, Alonso J A, Casais M T and Fernandez-Diaz M T 2002 *Eur. J. Inorg. Chem.* **9** 2463
[8] Rammeh N, Ehrenberg H, Fuess H and Cheikkh-Rouhou A 2006 *Phys. Status Solidi C* **3** 3225
[9] Hinatsu Y and Doi Y 2006 *J. Solid State Chem.* **179** 2079
[10] Pradheesh R, Nair H S, Kumar C M N, Lamsal J, Nirmala R, Santhosh P N, Yelon W B, Malik S K, Sankaranarayanan V and Sethupathi K 2012 *J. Appl. Phys.* **111** 053905
[11] Viola M C, Martínez-Lope M J, Alonso J A, Velasco P, Martínez J L, Pedregosa J C, Carbonio R E and Fernández-Díaz M T 2002 *Chem. Mater.* **14** 812
[12] Bezdicka P, Fournés L, Wattiaux A, Grenier J C and Pouchard M 1994 *Solid State Commun.* **91** 501
[13] Nomura K, Rykov A I, Nemudry A P and Mitsui T 2007 *Thin Solid Films* **515** 8645
[14] Bannikov V V, Shein I R, Kozhevnikov V L and Ivanovskii A L 2008 *J. Struc. Chem.* **49** 781
[15] Faik A, Gateshki M, Igartua J M, Pizarro J L, Insausti M, Kaindl R and Grzechnik A 2008 *J. Solid State Chem.* **181** 1759
[16] Augsburger M S, Viola M C, Pedregosa J C, Munoz A, Alonso J A and Carbonio R E 2005 *J. Mater. Chem.* **15** 993
[17] Ortega-San Martin L, Chapman J P, Lezama L, Sanchez-Marcos J, Rodriguez-Fernandez J, Isabel Arriortua M and Rojo T 2005 *J. Mater. Chem.* **15** 183
[18] Bull C L, Gleeson D and Knight K S 2003 *J. Phys.: Condens. Matter* **15** 4927
[19] Retuerto M, Martínez-Lope M J, García-Hernández M, Fernández-Díaz M T and Alonso J A 2008 *Eur. J. Inorg. Chem.* **4** 588
[20] Gateshki M, Igartua J M and Hernandez-Bocanegra E 2003 *J. Phys.: Condens Matter* **15** 6199
[21] Viola M C, Martinez-Lope M J, Alonso J A, Martinez J L, De Paoli J M, Pagola S, Pedregosa J C, Fernandez-Diaz M T and Carbonio R E 2003 *Chem. Mater.* **15** 1655
[22] Ivanov S A, Nordblad P, Mathieu R, Tellgren R and Ritter C 2010 *Dalton Trans.* **39** 11136
[23] Manoun B, Igartua J M, Gateshki M and Saxena S K 2008 *J. Mol. Struct.* **888** 244
[24] Lufaso M W, Gemmill W R, Mugavero S J III, Lee Y, Vogt T and Loye H C 2006 *J. Solid State Chem.* **179** 3556
[25] Wu H P, Qian Y, Tan W S, Xiao C Y, Deng K M and Lu R F 2011 *Appl. Phys. Lett.* **99** 123116
[26] Yang Y, Jiang Y S, Wang Y W and Sun Y B 2007 *J. Mol. Catal. A: Chem.* **270** 56
[27] Wang P, Yao L, Wang M and Wu W 2000 *J. Alloys Compd.* **311** 53
[28] Viret M, Ranno L and Coey J M D 1997 *Phys. Rev. B* **55** 8067
[29] Coey J M D, Viret M and Ranno L 1995 *Phys. Rev. Lett.* **75** 3910
[30] De Teresa J M, Ibarra M R, Blasco J, Garcia J, Marquina C and Algarabel P A 1996 *Phys. Rev. B* **54** 1187
[31] Birch F 1947 *Phys. Rev.* **71** 809